Results in Physics 19 (2020) 103364

Contents lists available at ScienceDirect

Results in Physics

journal homepage: www.elsevier.com/locate/rinp

The role of stirring time on the metallurgical and mechanical properties during modified friction stir clinching of AA6061-T6 and AA7075-T6 sheets

Shabbir Memon[a], Moslem Paidar[b,*], Olatunji O. Ojo[c], Kavian Cooke[d,*], Behzad Babaei[e], Mojtaba Masoumnezhad[f]

[a] Department of Mechanical Engineering, Wichita State University, Wichita, United States
[b] Department of Materials Engineering, South Tehran Branch, Islamic Azad University, Tehran, Iran
[c] Department of Industrial and Production Engineering, Federal University of Technology Akure, Akure, Nigeria
[d] Faculty of Engineering and Informatics, University of Bradford, Richmond Road, BD7 1DP Bradford, West Yorkshire, UK
[e] Department of Mechanical Engineering, Iran University of Science and Technology, Narmak, Tehran, Iran
[f] Department of Mechanical Engineering, Faculty of Chamran Guilan Branch, Technical and Vocational University (TVU), Tehran, Iran

ARTICLE INFO

Keywords:
Modified friction stir clinching
AA7075-T6 aluminum alloy
AA6061-T6 aluminum alloy
Stirring time
Mode fracture, Mechanical properties

ABSTRACT

In this study, the modified friction stir clinching process was successfully utilized to weld the AA7075-T6 to AA6061-T6 aluminum alloys. The approach of this study was to appraise the influence of the stirring time (6, 12, and 18 s) on the metallurgical and mechanical behavior of the welded samples. The microstructural study demonstrated that stirring time significantly affected joint properties and material flow, which can be ascribed to the discrepancy in the properties of the Al alloys used in this study. Void, local melting and defect-free joints were produced under the stirring times of 6 s, 18 s, and 12 s respectively. It was found that tensile/shear strength increased significantly from 63.5 MPa to 109 MPa as the stirring time increased from 6 s to 12 s, while a further increase in the stirring time to 18 s significantly decreased the joint's strength to 76.1 MPa. The observed failed samples showed that stirring time did not influence fracture mode.

Introduction

Aluminum and its alloys are marvelous lightweight metals that have found structural applications in the aerospace, naval and automotive industries owing to their good machinability, strength, and high corrosion resistance [1,2]. High-strength 7075 Al alloy is always employed for structural components ranging from airplane wings, panels, and aircraft fuselage [3]. Since the strength of 6061 Al alloy is satisfactory, the vast majority of industries such as high-speed trains industries use it as a vital structural alloy [3]. By conventional fusion welding techniques, the joining of Al alloys is considered problematic [2] due to several issues such as the creation of brittle and crispy phases, residual stresses, and solidification cracking [2,4]. In the 1990 s, the Friction stir welding (FSW) process was developed to join various metals, especially light metals such as magnesium (Mg) and aluminum (Al) alloys [5]. The peak temperature achieved during the FSW process is customarily lower than the parent materials' melting points [3]. To date, many experiments have been performed to explicate the metallurgical and mechanical behaviors of FSW joints [3,6,7]. Friction stir spot welding (FSSW) process was utilized in the car companies, in 2001, in replacement of the resistance spot welding of aluminum alloys [8–10]. The FSSW welded samples have been reported to have excellent metallurgical and mechanical properties, but an adverse tool-induced exit-hole is inevitable in the joints [1].

Multiple researchers have examined different processes for the elimination of keyhole in the FSSW welds [1,11–14]. In literature, eliminating keyhole strategies are based on the refilling of the keyhole through a substitute approach, which maintains the metallurgical superiority of the FSSW [1]. The design of a sophisticated tool is required for eliminating keyholes in the refilled FSSW process [15–18]. This is specifically noteworthy for the welding of dissimilar Al-Al sheets [1,19]. Many other novel welding techniques for spot welding have been reported in the literature. For instance, Liu et al. [20] reported that the application of friction stir spot riveting produced good metallurgical bonding and mechanical interlocking in Al/Cu joints. Huang et al. [21] investigated the friction filling staking joining process (of a metal-polymer joint) and it was revealed that the obtained tensile strength was comparable to that of other modern joining techniques. Other keyhole elimination processes that have been investigated in the literature include pin-plunging strengthened refill friction stir spot

* Corresponding authors.
E-mail addresses: m.paidar@srbiau.ac.ir (M. Paidar), K.Cooke1@bradford.ac.uk (K. Cooke).

https://doi.org/10.1016/j.rinp.2020.103364
Received 6 June 2020; Received in revised form 24 August 2020; Accepted 25 August 2020
Available online 24 September 2020

welding [22], double-sided friction stir spot welding [23], and friction spot extrusion welding [24].

Recent studies have shown several efforts in modifying the conventional FSSW method to eliminate pinhole from the weld structure. A pinless tool designed with a limited intermixing between the joining layers has more potential to be used for dissimilar welds [25–28]. The cheap design of the pinless tool not only can refill the pinhole but also can achieve a less diluted dissimilar bonding, which prevents the creation of the intermetallic compounds (IMCs) at the hybrid interface of the joints [29]. Following Paidar et al. [25], the MFSC process is a modification of the traditional friction stir clinching process where a 2-step approach is employed for the elimination of keyhole and protrusion. The MFSC method is different from the refill/pinless FSSW process as it employs two forms of tools (pin tool and pinless tool) with different shoulder diameters to improve materials movement from both sides of the MFSC joint [30]. Paidar et al. [19,25] examined the MFSC of the AA2024-T3 Al and AA7075-T6 Al alloys. They found that the tensile-shear and cross-tensile strengths of the welded AA2024-T3/AA6061-T6 samples improved by 83% and 50% respectively in comparison with the conventional friction stir spot welded joints in studies of Paidar et al. [1].

Hereupon, this study improves the modified friction stir clinched AA7075-T6 and AA6061-T6 joints' performance. The stirring time's impact on the metallurgical and mechanical properties is discussed. It is imperative to mention that this is the first work to appraise the welding of AA7075 to AA6061 with the MFSC process. Moreover, the mechanical properties, and also microstructure changes of the joints were evaluated to obtain the optimum stirring time for the joints strength.

Materials and methods

The materials employed in this work were AA7075-T6 and AA6061-T6 aluminum alloys with thicknesses of 2 mm and 1 mm, respectively. The mechanical properties and chemical analysis of these alloys are shown in Tables 1 and 2, respectively. Besides, the optical images of the as-received AA7075-T6 and AA6061-T6 aluminum alloys are presented in Fig. 1.

Before the welding process, the aforementioned alloys were cleaned with acetone solvent to erase the surface dust and paint upon the alloys. As shown in Fig. 2, a two-step modified friction stir clinching (MFSC) method was applied for joining the alloys. Before the start of the MFSC process, a pre-drilled blank hollow section was made in the backing anvil (upon which the overlapped workpieces were fixed) for the establishment of a plasticized protrusion during the first phase of the MFSC process. In the first phase of the MFSC procedure, a cylindrical pin tool was used (see Fig. 2a) to generate a mass protrusion on the bottom side of the welded joint while a pinhole is left at the upper side of the joint. The pin tool has a pin diameter, shoulder diameters, and a pin height of 10, 4, and 2.4 mm respectively. However, a pinless tool with a wider shoulder diameter (14 mm) was used to return the mass protrusion plastically into the hollow section made during the first phase of the MFSC procedure (see Fig. 2b).

In accordance with the outcomes of the primal tests, the specifications of tool rotational rate, shoulder drop depth and stirring time were constant for the first phase of the MFSC procedure (1250 rpm, 8 s and 0.4 mm) whereas varied stirring time from 6 s to 18 s was exerted over the second phase of the MFSC procedure. It should be declared that the second phase of the MFSC procedure (a pinless shoulder) was conducted at a constant rotational speed (1400 rpm) and penetration depth (0.4 mm). The welded samples were examined under a JEOL 6100 transmission electron microscope (TEM) and an optical microscope (Olympus BX51). To study the microstructure, the welded samples were electrolytically etched with a Barker agent (5 ml HBF_4 (25%) + 200 ml H_2O) for approximately 120 s and 25 V. The grain sizes of the joints were measured via the use of an image analyzer. In conforming to the JIS Z3136 standards, the tensile strength of the joints (see Fig. 3a) was carried out at a displacement speed of 1 mm min-1 by using an Intron 5500R general tensile experimenting gadget at room temperature. The schematic and dimensions of the MFSC welds are indicated in Fig. 3b and c.

Table 1
Mechanical properties of the parent alloys used in this work.

Alloy	Yield Strength [MPa]	Ultimate Tensile [MPa]	Elongation (%)
AA7075-T6	489	593	12
AA6061-T6	259	287	11

Table 2
Chemical composition of the parent alloys used in this work (wt.%).

Alloy	Al	Mg	Cu	Mn	Cr	Si
AA7075-T6	Base	2.26	1.68	0.13	0.28	0.12
AA6061-T6	Base	0.87	0.21	0.056	0.104	0.61

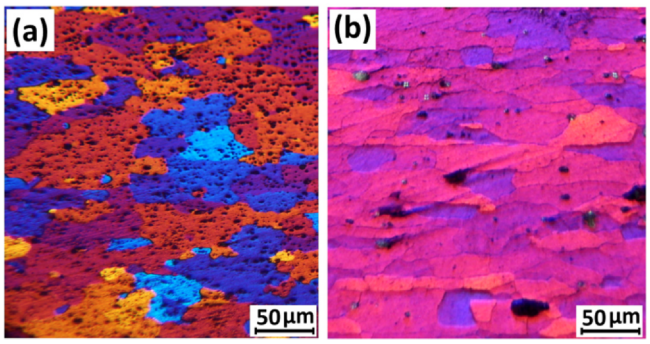

Fig. 1. As-received microstructure of the (a) AA7075-T6 and (b) AA6061-T6.

Results and discussion

The surface appearances of welded samples after the MFSC process as a function of stirring time at the AA6061-T6 side are represented in Fig. 4a-c. It is considerably apparent that defect-free keyhole refilling is gained in all MFSC welded specimens, regardless of the level of stirring time. It is important to mention that the top views of the welds depict one kind of geometric-differential-flow imperfection at the circumferential edges of the weld nuggets, which can be attributed to the shoulder-induced cavity refilling effect that was produced during the 2nd phase of MFSC process [30]. Supplementary to this, the keyhole was produced by the retraction of the rotating tool during the 1st phase of the welding process, and it was eliminated during the second step of the MFSC process in the joints.

Fig. 4a represents the surface appearance of the MFSC joint having a shallow imperfectly filled circumferential defect at the weld centre (at stirring time 6 s). In contrast, with prolonged stirring time to 18 s, a keyhole-protuberance profile has been eliminated (see Fig. 4c). It can be concluded that stirring time played a pivotal role in eliminating the keyhole defect during the MFSC process. This depicts that the level of the keyhole-spacing at the centre of the welds diminishes, as the stirring time is increased from 6 s to 18 s. Paidar et al. [25] have reported that an amalgamation of an increase in both tool rotational rate and shoulder plunge depth was appropriate in removing the flow-induced key-hole defect and shoulder cavitation in the MFSC of 2024-T3-7075-T6 spot weld.

Fig. 4d illustrates the surface appearance (top view) of the traditional FSSW. As it is obvious, the presence of keyhole on the surface of the conventional FSSW joint, owing to the retraction of the cylindrical pin tool. Paidar et al. [19] examined the possibility of MFSC of 2024/

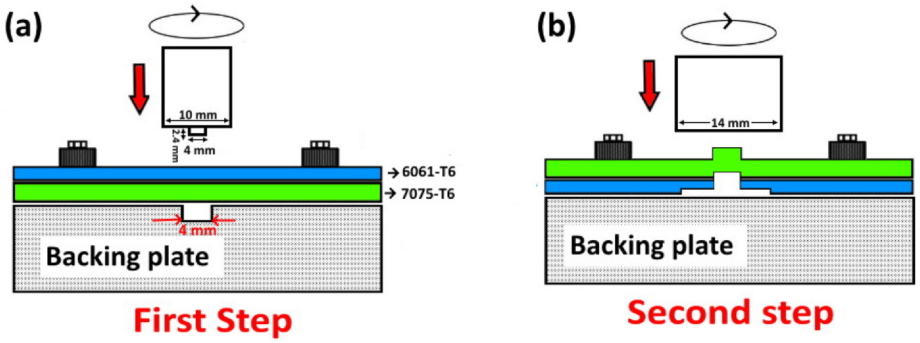

Fig. 2. MFSC welding procedure for 6061-T6/7075-T6 joints (a) first step; (b) second step of MFSC.

7075 sheets. Their results depicted that the complete elimination of keyhole enhanced the bonding area and subsequently led to the betterment of the fracture strength of the welded joint. Fig. 4e shows the bottom view of the sample with a pinless shoulder tool at the AA7075-T6 side during the 2nd phase of the MFSC process.

The joint morphology of the AA6061-T6/AA7075-T6 dissimilar welds as a function of stirring time has been shown in Fig. 5. These images confirm the complete removal of keyhole and intermingling between Al alloys by increasing the stirring time during the MFSC process. This incidence indicates that the pin-induced keyhole is successfully filled at the AA6061-T6 side irrespective of the stirring time. This occurrence is owing to the enhancement in deformational induced heat-input, better flowability, and material flow within the weld nugget from the AA7075-T6 side to AA6061-T6 side at higher stirring times. The imperfectly refilled area (beneath the shoulder) and weld thinning are attributed to insufficient geometric differential flow and shoulder plunging effects respectively [31]. These defects will reduce the load-bearing area and induce stress concentrations on the samples obtained at 6 s. However, small voids were observed at 6 s stirring time. This manifestation indicates that 6 s stirring time was insufficient for MFSC of AA6061 to AA7075-T6.

This is also evident in Fig. 5 (see the blue ovals in Fig. 5), increasing in the level of stirring time resulted in the better stirring of materials and accordingly, a wider bonded width at the AA7075-T6 side. This confirmed the significant effect of the 2nd step of the welding (MFSC) process with a pin-less tool for keyhole elimination. Hence, the shoulder-induced cavitation on the AA6061-T6 side (see the red rectangular in Fig. 5) is at the shoulder edges (circumferential), creating a refilling challenge. Also, this can substantially influence the process parameter combination [19] and the severity of the inter-material mixing features [1]. These results confirmed the complete removal of keyhole after the second step of MFSC and showed a better intermingling between Al alloys by increasing the stirring time from 6 s to 18 s. Indeed, a rise in stirring time is adjudged to have enhanced material flow. However, micro-voids and cracks were obtained in the joint at the high stirring time.

This occurrence has been ascribed to the heat input emanating from the friction-deformation effects owing to the prolonged stirring time and diversity in materials flow of Al alloys at shoulder-induced boundary [1].

In Fig. 6, SEM-backscattered electron image of defects (at the weld centres) has been shown, which is correlated with material flow conditions. As it is obvious in Fig. 6, various layers and interface voids revealed clearly during the MFSC of AA7075/6061-T6. Indeed, Fig. 6 confirmed the considerable effect of the tool stirring time on the frictional heat, and consequently, a significant improvement in the flowability of the base alloys occurs at a higher stirring time. Gerlich et al. [32] discovered that the reason behind this occurrence could be originated from frictionally induced peak temperature, which caused the natural melting temperatures of the second particles in the AA7075 alloy. They have found that the natural melting at the inter-grain border area caused the production of molten eutectic phases and subsequently resulted in cracking at the area under the instrument tip.

As can be seen in Fig. 6a, voids are created in low stirring time, whereas cracks were found clearly in SZ at a high stirring time (18 s). The process can be due to the local melting of the Al_2CuMg (S) phase

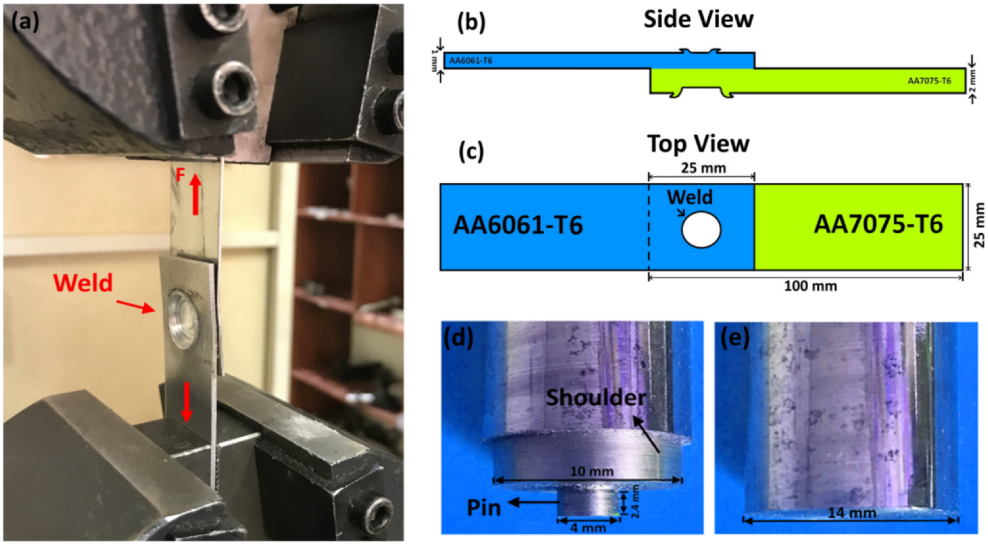

Fig. 3. (a) Tensile/shear Machine. (b) and (c) The schematic and dimensions of the Tensile/shear test. The tools used in the (d) first step and (e) second step.

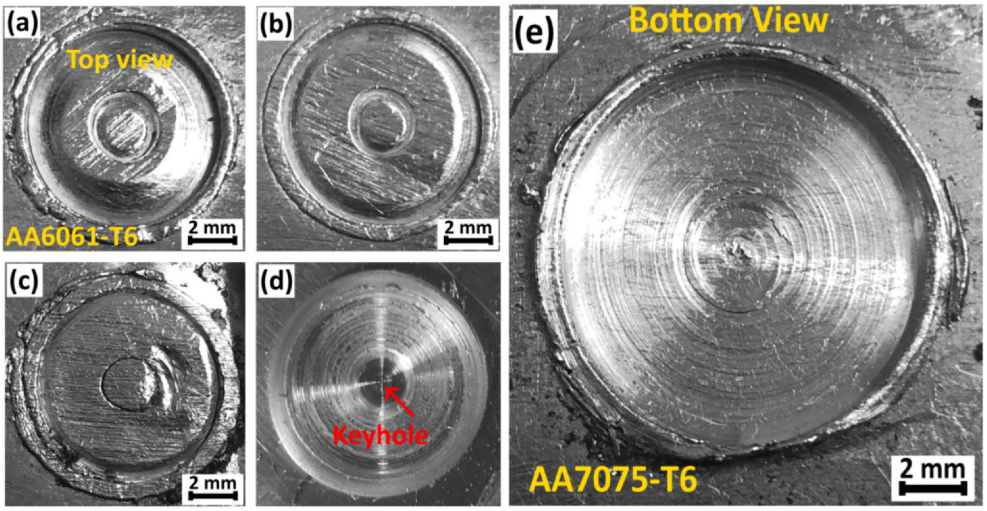

Fig. 4. Surface appearance of welds, (a) 6 s, (b) 12 s, (c) 18 s, (d) Conventional FSSW (Top view), (e) Bottom view of MFSC.

[33,34], which has a melting temperature of 490 °C, $Al_6CuFeMn$ [32], or Al_2Cu (Θ) phase within the solidified weld matrix. In accordance with the EDS results, these crack consisted of Mg, Cu, Zn, and Mn (see Fig. 6d). As it is provided in the Appendix A1, the dispersion (inter-material mixing level) within the SZ is provided in the EDS mapping. The results of EDS analysis of locations A, B, and C are listed in Table 3.

The magnified structures within the MFSC AA7075-T6/AA6061-T6 joints obtained at different tool stirring times are shown in Fig. 7. It can be observed in Fig. 7 that the level of material mixing is improved as the stirring time is increased. Evidence of improperly mixed material flow-path is observed at a lower stirring time while considerably mixed zone ensues at a higher stirring time (18 s stirring time). This observation is owing to the impact of frictional heat input on material flowability, better material mixing, and transport at a higher stirring time [35].

In addition to the mentioned point, adequate inter- substance blending produced complete metallurgical connection in the joint. The adequate heat input, which is needed for increased flowability and movement of material from the AA7075 to AA6061 and vice versa, was responsible for this behavior when the stirring time was raised from 6 s to 18 s. Nevertheless, it appears that when the stirring time of the tool increased to 18 s (see Fig. 7), complete metallurgical observation is evident in the area around the center of the weld. In contrast, the un-completed metallurgical connection proceeds toward the sides of the joint (see Fig. 7b). Fig. 7c confirmed the complete elimination of defect associated with material flow at 6 s stirring time for the MFSC joints despite the varied stirring times, whereas local melting was occurred in welded jointed at 18 s stirring time as it is indicated in Fig. 7b. In accordance with this result, it can be concluded that sufficient inter-material mixing and metallurgical bonding ensue with prolonged stirring time during the MFSC process. Furthermore, it can be concluded that the mixing rate in the joint depends on stirring time, and 6 s stirring time indicates weak intensity for the welded samples. In other words,

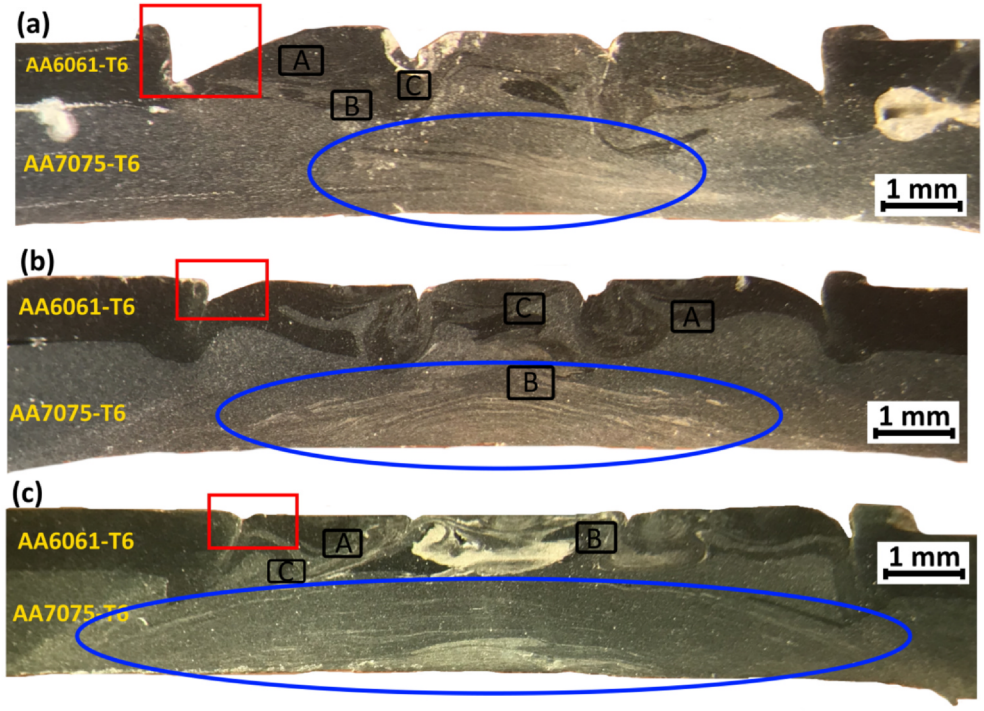

Fig. 5. Macrostructure of welded produced at various stirring times, (a) 6 s, (b) 12 s, and (c) 18 s.

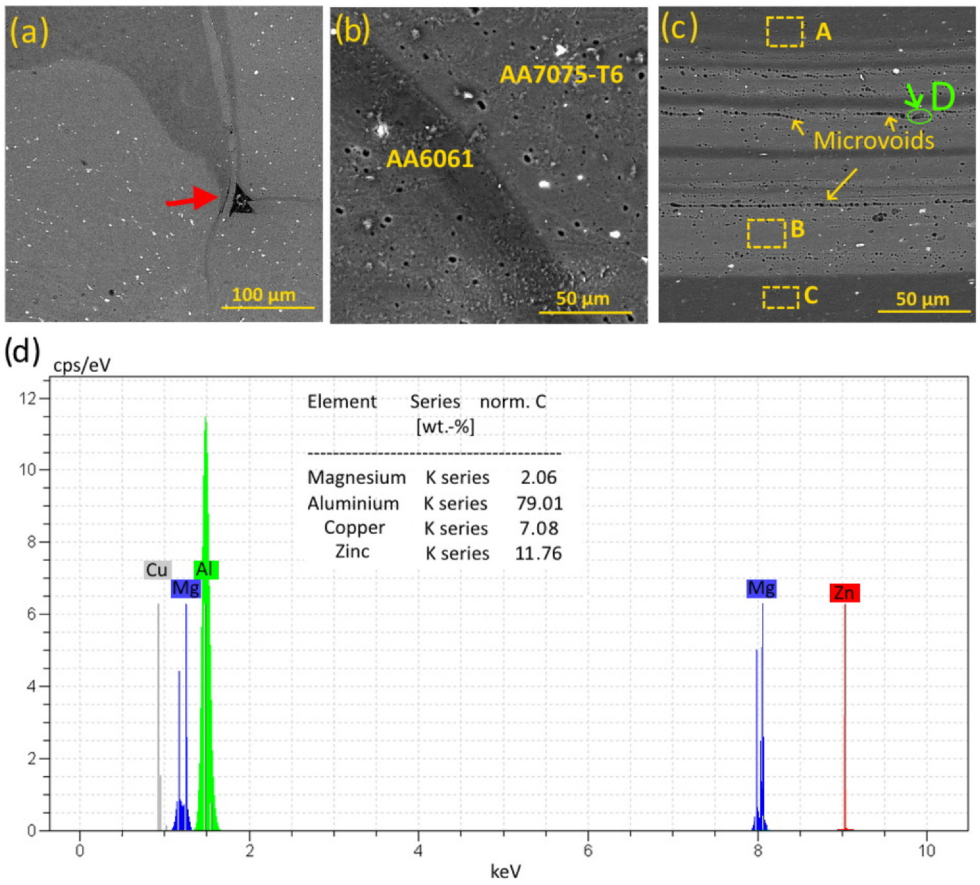

Fig. 6. SEM images of welded produced at various stirring times, (a) 6 s, (b) 12 s, (c) 18 s, (d) EDS result of location D in Fig. 3c.

Table 3
EDS results of locations A, B, and C.

Location	Al	Cu	Mg	Zn	Si	Fe
A	96.35	0.66	1.39	–	0.82	0.74
B	89.65	2.61	1.79	5.95	–	–
C	95.23	0.48	1.61	2.19	0.28	0.21

increasing the stirring time can cause an increase in the average grains, more growth, and elongation of the grains in all regions. When the stirring time was increased from 6 s to 18 s, the inter-material mixing and the heat input induced during the MFSC process was intensified and this subsequently facilitated the possibility of cracking in the welded joints, especially in the SZ.

Fig. 8 presents the SZ and TMAZ structures of the welded joints as a function of stirring times. From Fig. 8, it is obvious that the SZ structures have equiaxed grains regardless of the stirring time. It is clear that at longer stirring times, equiaxed large grains are present at the SZ but the assessment of the grain sizes is necessary. An increase in the stirring time (from 6 s to 12 s) increases the (average) grain sizes of the joints from 5.39 to 6.35 µm whilst after 18 s, the grain size of SZ further increases to 7.89 µm. The severe plastic deformation at the weld nugget zone or SZ leads to the formation of fine and homogeneous equiaxed crystals due to the dynamic recrystallization (DRX) phenomenon at the SZ. Padhy et al. [36] revealed that fine grains are produced in the SZ of the welds. They have reported that the probable reasons for this occurrence are the strain-aided rotation of subgrains (through absorption of dislocation), improved transformation, and misorientation.

Fig. 8b depicts the TMAZ structure on the AA6061-T6 side. It should be noted that when a further increase in stirring time is applied, stretched/elongated grains were obtained due to the thermo-mechanical impact of the welding process. As it was expected, the severity of the inter-mixing in the TMAZ increases with the increase in the level of stirring time, whereas slightly elongated grains are observed at a lower stirring time (6 s).

The supplementary studies for investigating the effects of the grain refinement and the precipitation mechanism require an accurate observation in higher magnification, which is provided by the electron microscopy, e.g., the TEM technique. Fig. 9 displays the as-welded joints' Bright Field TEM images at the 18 s stirring time. By high-resolution TEM micrograph, the results of the structural study indicate that more fine secondary phases are formed in the weld zone [1]. This phenomenon could be related to deformation-induced fragmentation, and in fact, a better distribution of particles occurred at the stir zone of the joint (see blue arrows). Evidence of precipitated phases and low dislocation density is observed in the as-welded joint owing to the dissolved strengthening phases in the joint. Braun et al. [37] discovered that there is a direct correlation between the fracture load, dissolution, and growth of the precipitates. The results of the study indicated that more stirring time increased dislocation density. Tran et al. [38] noted that the intense overexert alters dislocation walls to sub-grains, the whole energy condition in the grains is decreased.

The dislocation network around the substrate particles formed a sub-grain boundary network to compensate for the induced strain through the grain lattice, which is caused by the precipitation. The stored strain which is induced by the severe plastic deformation and the subsequent frictional heat generation has acted as the main driving force in nucleation precipitation.

The outcomes of the tensile/shear tests with stress–strain curves and subsequently fractured surfaces for the failed welds are illustrated in Fig. 10. As it is clear, increasing the stirring time from 6 s to 12 s efficiently increases the maximum fractured load from 63.5 MPa to about

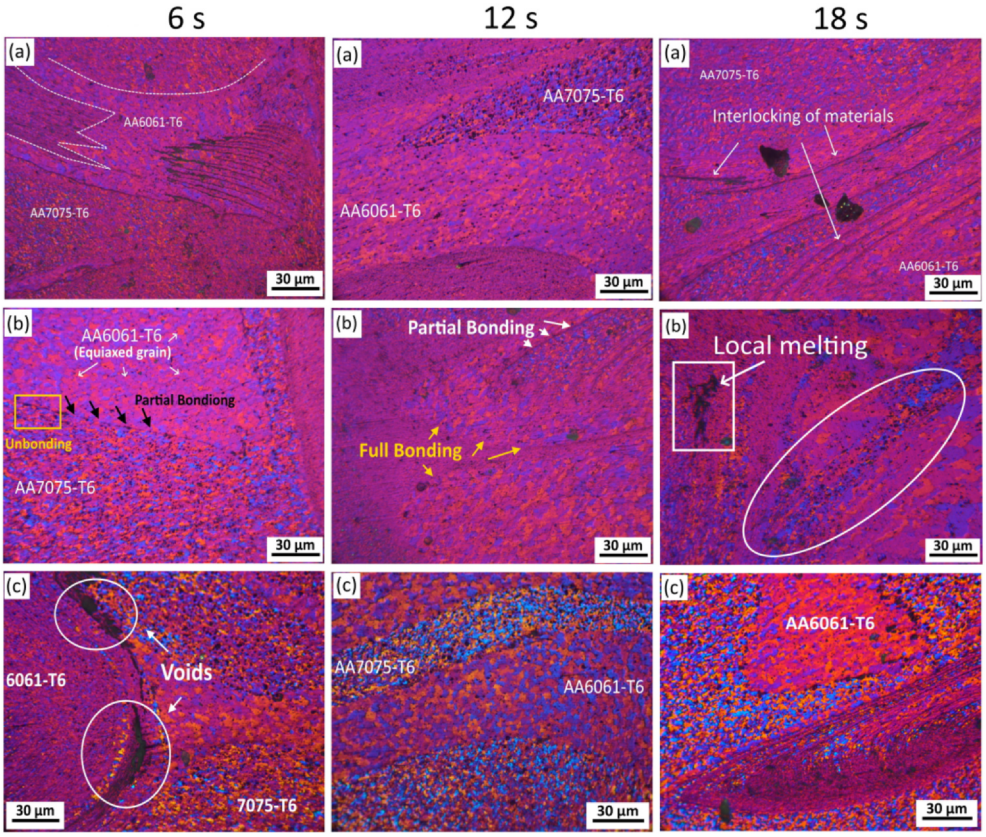

Fig. 7. Optical images of different locations within the weld as a function of stirring time at various zones, (a) Center of SZ.

109 MPa. Indeed, it can be said that because of better material flow/interblending needed for adequate metallurgical connection, the fracture load value increases. Paidar et al. [17,23] revealed that the main reason for the increase in the joint strength of the MFSC AA2024-T3/AA7075-T6 joint was the advancement in the connection mechanism and efficient bonded/shear region. It should be declared that when a further increase in stirring time is applied (18 s), the maximum fractured load decreased to 76.1 MPa. This occurrence is mainly attributed to defects (local melting) caused by the local melting of the AA7075-T6 Al alloy in the weld nugget due to the generated heat input connected to long stirring time. Subsequently, this reduced the ultimate strength and hence culminated to lower fracture load in comparison with the welds without defect, which was obtained at 12 s stirring time. It can be inferred that the stirring time had a bilateral result on the tensile shear load. According to these outcomes, it can be summarized that stirring time can efficiently increase the fracture load/strength of the MFSC joints.

The schematic of the fracture path of the MFSC 6061/7075 welds is indicated in Fig. 11a-c. Indeed, Fig. 11a-c compares the effect of the stirring time on the fracture mode. Stirring time did not have a significant impact on the fracture mode of the welded joints under tensile/shear loading. Circumferential fracture mode is observed in all-welded samples regardless of the stirring time. Paidar et al. [23] reported that the MFSC welding parameters have a substantial influence on fracture mode of the spot welds. It can be observed that the crack initiated at the interface between AA7075 and AA6061 sheets, and propagated through the AA6061 aluminum alloy during loading irrespective of the tool stirring time. Nugget rotation is the phenomenon responsible for the observed fracture behavior in the works of Paidar et al. [1]. The fracture surfaces of the 6061/7075 MFSC welds obtained at the stirring time of 12 s are represented in Fig. 11 d-g. This indicates the predominance of ductile fracture behavior irrespective of the stirring time. As discussed earlier, stirring time did not affect the fracture mode. The presence of shallow dimples indicates that the welded joints failed via ductile fracture-mode.

Conclusion

Modified friction stir clinching of AA7075-T6 to AA6061-T6 aluminum sheets has been successfully carried out. The effect of stirring time on metallurgical and mechanical properties is investigated. About this research, the main conclusions are drawn as below:

i. Stirring time played a pivotal role to accomplish a sound MFSC weld. It was also beneficial for obtaining a preferable intermixing (interlocking) between the dissimilar materials during the MFSC process.
ii. At low stirring time, the MFSC welding process resulted in the creation of superficial geometric-differential flow faults at the shoulder-induced cavitation and replenished ends of the keyhole.
iii. The stirring time also modified the internal intermixing of the materials during the MFSC process; however, some defects were formed at lower and higher stirring times.
iv. Stirring time alters the material flow behavior of the MFSC joints by affecting the microstructure of SZ, TMAZ, and HAZ. A rise in stirring time from 6 s to 18 s increases the average grain sizes in SZ from 5.39 µm to 7.89 µm.
v. The stirring time had a bilateral effect on the tensile/shears strength. Tensile/shear strength increased significantly from 63.5 MPa to 109 MPa with increasing the stirring time from 6 s to 12 s, whilst when a further increase in stirring time is applied (18 s), the strength significantly decreased to 76.1 MPa.

CRediT authorship contribution statement

Shabbir Memon: Data curation. **Moslem Paidar:** Methodology.

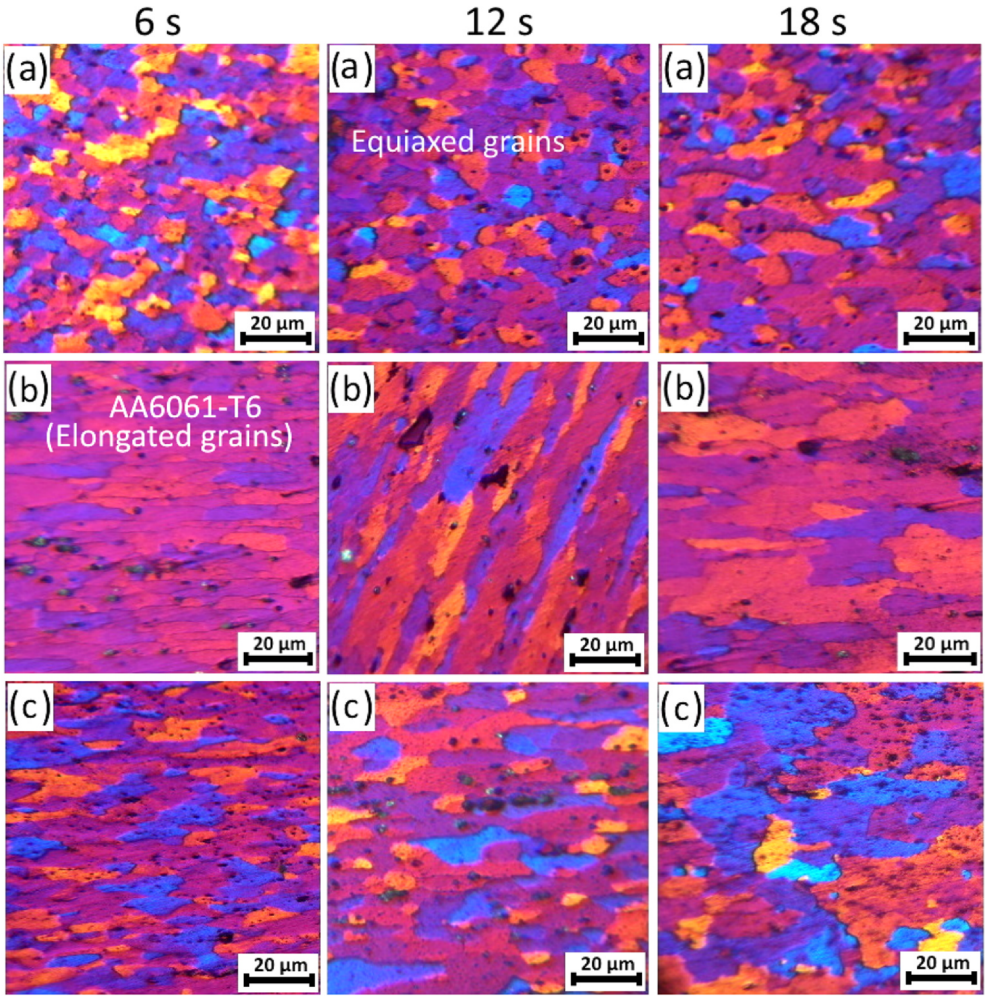

Fig. 8. Structure of various zones as a function of stirring time, (a) SZ (7075 side), (b) TMAZ (6061 side) and (c) TMAZ (7075 side).

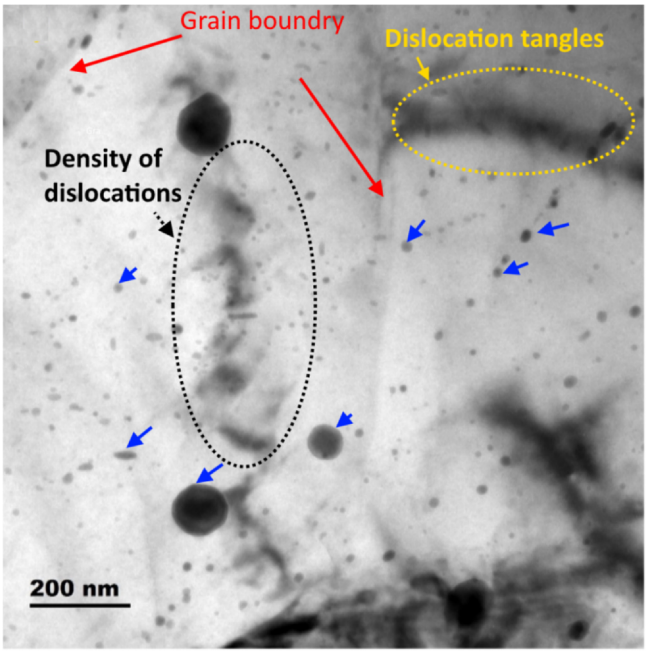

Fig. 9. TEM micrograph of MFSC AA7075-T6/AA6061-T6 joint (stir zone).

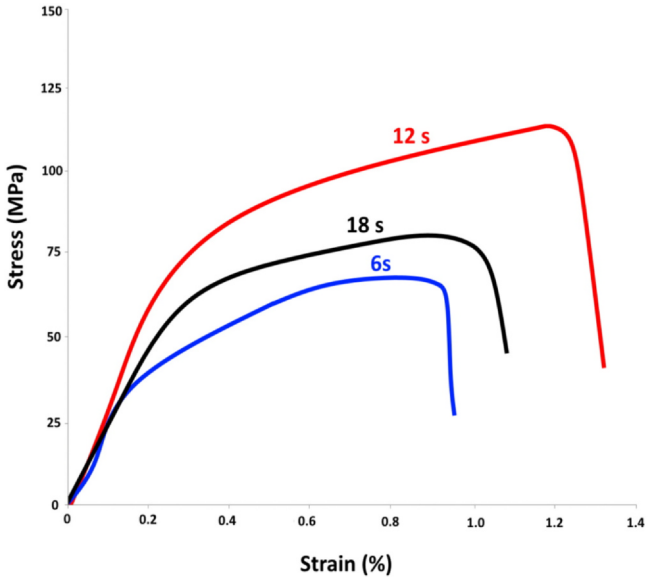

Fig. 10. (a) Stress-Strain curve as a function of stirring time.

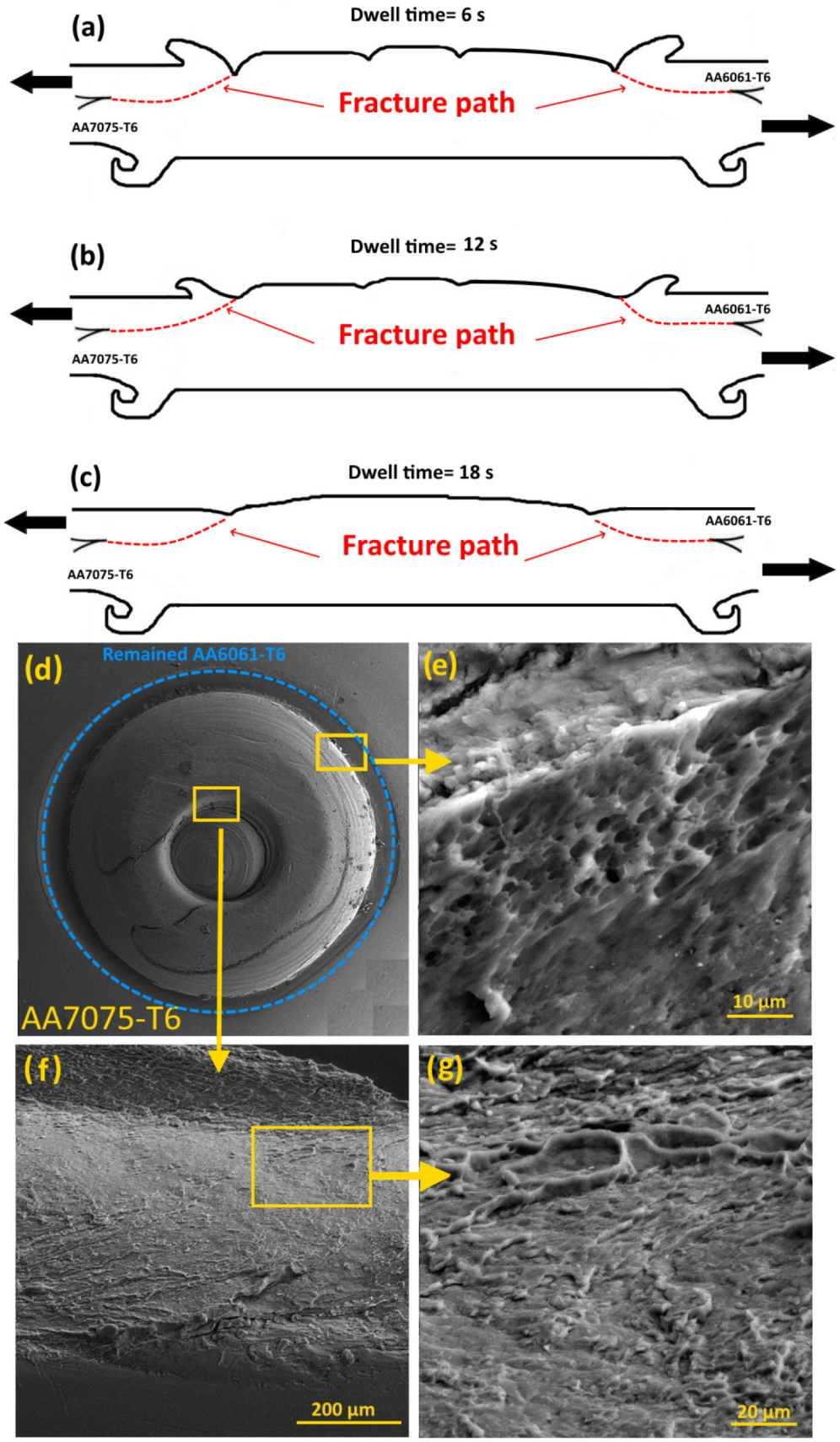

Fig. 11. (a) Schematic of the fracture path at 6 s and 18 s stirring time (the arrows show loading direction), (d)-(g) SEM image of the fracture surface of MFSC 6061/7075 spot weld produced at 12 s.

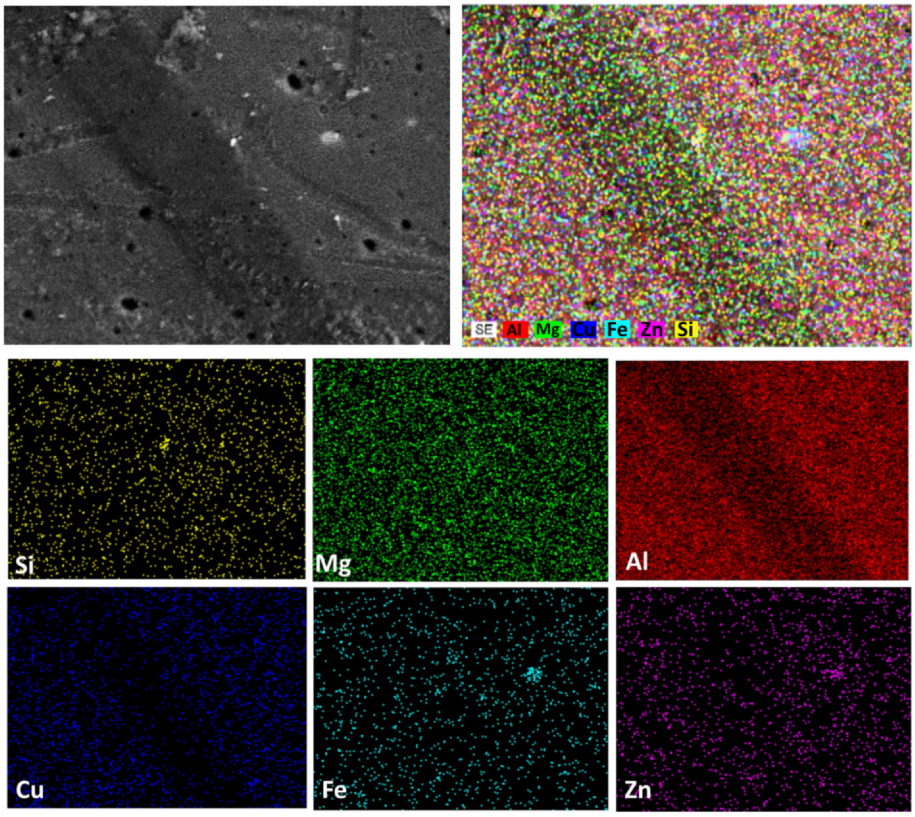

Fig. A1. EDS mapping of the MFSC 6061-T6/7075-T6 joint.

Olatunji O. Ojo: Project administration, Writing - original draft. **Kavian Cooke:** Project administration, Writing - original draft. **Behzad Babaei:** Resources, Validation, Visualization. **Mojtaba Masoumnezhad:** Investigation, Writing - review & editing.

Declaration of Competing Interest

The authors declare the following financial interests/personal relationships which may be considered as potential competing interests: Shabbir Memon: Department of Mechanical Engineering, Wichita State University, Wichita, United States, Moslem Paidar: Department of Materials Engineering, South Tehran Branch, Islamic Azad University, Tehran 14598-53849, Iran, O. Ojo: Department of Industrial and Production Engineering, Federal University of Technology Akure, Nigeria, Kavian Cooke: Faculty of Engineering and Informatics, University of Bradford, Richmond Road, BD7 1DP, Bradford, West Yorkshire, UK, Behzad Babaei: Department of Mechanical Engineering, Iran University of Science and Technology, Narmak, Tehran, Iran, Mojtaba Masoumnezhad: Department of Mechanical engineering, Faculty of Chamran Guilan Branch, Technical and Vocational University (TVU), Tehran, Iran.

Appendix

Fig. A1.

References

[1] Paidar M, Vaira Vignesh R, Moharrami A, Ojo OO, Jafari A, Sadreddini S. Development and characterization of dissimilar joint between AA2024-T3 and AA6061-T6 by modified friction stir clinching process. Vacuum 2020;176:109298.
[2] Rodriguez RI, Jordon JB, Allison PG, Rushing T, Garcia L. Microstructure and mechanical properties of dissimilar friction stir welding of 6061-to-7050 aluminum alloys. Mater Des 2015;83:60–5.
[3] Liu Z, Yang K, Yan D. Refill friction stir spot welding of dissimilar 6061/7075 aluminum alloy. High Temp Mater Proc 2019;38:69–75.
[4] Gibson BT, Lammlein DH, Prater TJ, Longhurst WR, Cox CD, Ballun MC, et al. Friction stir welding: process, automation, and control. J Manuf Process 2014;16:56–73.
[5] Karami Pabandi H, Jashnani HR, Paidar M. Effect of precipitation hardening heat treatment on mechanical and microstructure features of dissimilar friction stir welded AA2024-T6 and AA6061-T6 alloys. J Manuf Processes 2018;31:214–20.
[6] Zhongjie Y, Xuesong L, Hongyuan F. Effect of sheet configuration on microstructure and mechanical behaviors of dissimilar Al-Mg-Si/Al-Zn-Mg aluminum alloys friction stir welding joints. J Mater Sci Technol 2016;32:1378–85.
[7] Buffa G, Fratini L, Schneider M, Merklein M. Micro and macro mechanical characterization of friction stir welded Ti–6Al–4V lap joints through experiments and numerical simulation. J Mater Process Technol 2013;213:2312–22.
[8] Paidar M, Vaira Vignesh R, Khorram A, Oladimeji Ojo O, Rasoulpouraghdam A, Pustokhina I. Dissimilar modified friction stir clinching of AA2024-AA6061 aluminum alloys: Effects of materials positioning. J Mater Res Technol 2020;9:6037–47.
[9] Paidar M, Laali Sarab M. Friction stir spot welding of 2024–T3 aluminum alloy with SiC nanoparticles. J Mech Sci Technol 2016;30:365–70.
[10] Paidar M, Khodabandeh A, Lali Sarab M, Taheri M. Effect of welding parameters (plunge depths of shoulder, pin geometry, and tool rotational speed) on the failure mode and stir zone characteristics of friction stir spot welded aluminum 2024–T3 sheets. J Mech Sci Technol 2015;29:4639–44.
[11] Tozaki Y, Uematsu Y, Tokaji K. A newly developed tool without probe for friction stir spot welding and its performance. J Mater Process Technol 2010;210:844–51.
[12] Lee C-J, Lee S-H, Lee J-M, Kim B-H, Kim B-M, Ko D-C. Design of hole-clinching process for joining CFRP and aluminum alloy sheet. Int J Precis Eng Manuf 2014;15:1151–7.
[13] Venukumar S, Yalagi S, Muthukumaran S, Kailas S. Static shear strength and fatigue life of refill friction stir spot welded AA 6061–T6 sheets. Sci Technol Weld Joining 2014;19:214–23.
[14] Chen K, Liu X, Ni J. Keyhole refilled friction stir spot welding of aluminum alloy to

advanced high strength steel. J Mater Process Technol 2017;249:452–62.
[15] Peng Li Su, Chen HD, Ji Ha, Li Y, Guo X, Yang G, et al. Interfacial microstructure and mechanical properties of dissimilar aluminum/steel joint fabricated via refilled friction stir spot welding. J Manuf Processes 2020;49:385–96.
[16] Shen Z, Li WY, Ding Y, Hou W, Liu XC, Guo W, et al. Material flow during refill friction stir spot welded dissimilar Al alloys using a grooved tool. J Manuf Processes 2020;49:260–70.
[17] Wang S, Wei X, Xu J, Hong J, Song X, Yu C, et al. Strengthening and toughening mechanisms in refilled friction stir spot welding of AA2014 aluminum alloy reinforced by graphene nanosheets. Mater Des 2020;186:108212.
[18] Li P, Chen S, Dong H, Ji H, Li Y, Guo X, et al. Interfacial microstructure and mechanical properties of dissimilar aluminum/steel joint fabricated via refilled friction stir spot welding. J Manuf Processes 2020;49:385–96.
[19] Paidar M, Ojo OO, Moghanian A, Karapuzha AS, Heidarzadeh A. Modified friction stir clinching with protuberance-keyhole levelling: A process for production of welds with high strength. J Manuf Processes 2019;41:177–87.
[20] Liu J, Song Q, Song L, Ji S, Li M, Jia Z, et al. A novel friction stir spot riveting of Al/Cu dissimilar materials. Acta Metall Sinica (English Letters) 2020. https://doi.org/10.1007/s40195-020-01092-2.
[21] Huang Y, Meng X, Xie Y, Li J, Wan L. New technique of friction-based filling stacking joining for metal and polymer. Compos B Eng 2019;163:217–23.
[22] Cao JY, Zhang CC, Xing YF, Wang M. Pin plunging reinforced refill friction stir spot welding of Alclad 2219 to 7075 alloy. J Mater Process Technol 2020;284:116760.
[23] Cox CD, Gibson BT, DeLapp DR, Strauss AM, Cook GE. A method for double-sided friction stir spot welding. J Manuf Processes 2014;16:241–7.
[24] Han J, Paidar M, Vaira Vignesh R, Mehta KP, Heidarzadeh A, Ojo OO. Effect of shoulder features during friction spot extrusion welding of 2024–T3 to 6061–T6 aluminum alloys. Archiv Civil Mech Eng 2020;20:1–17.
[25] Paidar M, Ghavamian S, Ojo OO, Khorram A, Shahbaz A. Modified friction stir clinching of dissimilar AA2024-T3 to AA7075-T6: Effect of tool rotational speed and penetration depth. J Manuf Processes 2019;47:157–71.
[26] Ojo OO, Taban E, Kaluc E. Effect of residual Alclad on friction stir spot welds of AA2219 alloys. Mater Test 2018;60:979–88.
[27] Li W, Li J, Zhang Z, Gao D, Wang W, Dong C. Improving mechanical properties of pinless friction stir spot welded joints by eliminating hook defect. Mater Des 2014;62:247–54.
[28] Oladimeji OO, Taban E, Kaluc E. Understanding the role of welding parameters and tool profile on the morphology and properties of expelled flash of spot welds. Mater Des 2016;108:518–28.
[29] Mehta KP, Patel R, Vyas H, Memon S, Vilaça P. Repairing of exit-hole in dissimilar al-mg friction stir welding: Process and microstructural pattern. Manuf Lett 2020.
[30] Paidar M, Tahani K, Vaira Vignesh R, Ojo OO, Ezatpour HR, Moharrami A. Modified friction stir clinching of 2024-T3 to 6061-T6 aluminum alloy: Effect of dwell time and precipitation-hardening heat treatment. Mater Sci Eng A 2020;791:139734.
[31] Meng X, Huang Y, Cao J, Shen J, dos Santos JF. Recent progress on control strategies for inherent issues in friction stir welding. Prog Mater Sci 2021;115:100706.
[32] Su P, Gerlich A, North TH, Bendzsak GJ. Intermixing in dissimilar friction stir spot welds. Mater Trans 2007;38:584–95.
[33] Brooks CR. Heat treatment structure and properties of nonferrous alloys. Am Soc Met 1982;4:115–39.
[34] Paidar M, Khodabandeh A, Najafi H, Sabour Rouh-aghdam A. Effects of the tool rotational speed and shoulder penetration depth on mechanical properties and failure modes of friction stir spot welds of aluminum 2024–T3 sheets. J Mech Sci Technol 2014;28:4893–8.
[35] Ebrahimzadeh V, Paidar M, Safarkhanian MA, Oladimeji Ojo O. Orbital friction stir lap welding of AA5456-H321/AA5456-O aluminum alloys under varied parameters. Int J Adv Manuf Technol 2018;96:1237–54.
[36] Padhy GK, Wu CS, Gao S. Friction stir based welding and processing technologies - processes, parameters, microstructures, and applications: A review. J Mater Sci Technol 2018;34:1–38.
[37] Braun R, Dalle C, Staniek DG. Laser beam welding and friction stir welding of 6013–T6 aluminum alloy sheet. Mater Sci Eng Technol 2000;31:1017–26.
[38] Tran V-X, Pan J, Pan T. Effects of processing time on strengths and failure modes of dissimilar spot friction welds between aluminum 5754-O and 7075–T6 sheets. J Mater Process Technol 2009;209:3724–39.